CXCR4-Directed Imaging and Endoradiotherapy in Desmoplastic Small Round Cell Tumors

Ingo Hartlapp*[1], Philipp E. Hartrampf*[2], Sebastian E. Serfling[2], Vanessa Wild[3], Alexander Weich[1], Leo Rasche[1], Sabine Roth[3], Andreas Rosenwald[3], Patrick W. Mihatsch[4], Anne Hendricks[5], Armin Wiegering[5], Verena Wiegering[6], Heribert Hänscheid[2], Andreas Schirbel[2], Rudolf A. Werner[2], Andreas K. Buck[2], Hans-Jürgen Wester[7], Hermann Einsele[1], Volker Kunzmann[1], Constantin Lapa*[8], and K. Martin Kortüm*[1]

[1]Department of Internal Medicine II, Medical Oncology and Comprehensive Cancer Center Mainfranken, University Hospital Würzburg, Würzburg, Germany; [2]Department of Nuclear Medicine and Comprehensive Cancer Center Mainfranken, University Hospital Würzburg, Würzburg, Germany; [3]Department of Pathology and Comprehensive Cancer Center Mainfranken, University of Würzburg, Würzburg, Germany; [4]Department of Diagnostic and Interventional Radiology and Comprehensive Cancer Center Mainfranken, University Hospital Würzburg, Würzburg, Germany; [5]Department of General, Visceral, Transplantation, Vascular, and Pediatric Surgery and Comprehensive Cancer Center Mainfranken Würzburg, University Hospital Würzburg, Würzburg, Germany; [6]Children's Hospital and Comprehensive Cancer Center Mainfranken, University of Würzburg, Würzburg, Germany; [7]Pharmaceutical Radiochemistry, Technical University Munich, München, Germany; and [8]Nuclear Medicine, Medical Faculty, University of Augsburg, Augsburg, Germany

For correspondence or reprints, contact Martin Kortüm (kortuem_m@ukw.de).
*Contributed equally to this work.

Desmoplastic small round cell tumor (DSRCT) is an extremely rare malignant mesenchymal neoplasm that predominantly affects young men (*1*). The primary location is the abdominal cavity, in which is commonly found a multinodular disease affecting the omentum, retroperitoneum, and mesentery. Histologically, DSRCT is an aggressive sarcoma subtype that presents with multiphenotypic differentiation, including epithelial, muscular, and neural features, such as coexpression of cytokeratins, desmin, and synaptophysin. The recurrent balanced chromosomal translocation t(11:32)(p13;q12) is a pathognomonic hallmark and a driver of the disease. The corresponding EWSR1-WT1 fusion gene codes for a chimeric protein, with typically strong nuclear expression, containing the N-terminal domain of the Ewing sarcoma breakpoint region 1 protein and 3 of the 4 zinc finger domains of the Wilms tumor 1 protein (*2,3*).

DSRCT is characterized by immunologic ignorance (*4*). In particular, next-generation sequencing molecular profiling revealed a paucity of secondary mutations with notable heterogeneity between patients, and (except for FGFR4 mutations in only a small subset of patients), no suitable therapeutic targets could be identified (*5*).

Because of the lack of clinical trials in this orphan disease, with approximately 1,000 patients reported to date, no standard therapy has been established. Patients with DSRCT have been compiled in sarcoma studies, and systemic chemotherapy regimens are derived from protocols established primarily for Ewing and other soft-tissue sarcomas. Complete resection has been shown to increase overall survival (OS) (*6*); however, as primary curative surgery is rarely achievable, multimodal treatment with aggressive induction with or without high-dose chemotherapy with autologous stem cell transplantation followed by cytoreductive surgery with or without hyperthermic intraperitoneal chemotherapy (*7*) or whole-abdominal radiotherapy has been proposed (*2,3*). However, patients experience early relapse and prognosis remains poor, with a median OS

of 24–29 mo and 3-y and 5-y survival rates of 30%–35% and 4%, respectively (*8–10*). So far, targeted therapies with sunitinib (*11*) and pazopanib (*12,13*), as well as immunotherapy with nivolumab (*14*) or pembrolizumab, have demonstrated only limited effects (*15,16*).

Functional imaging using [^{18}F]FDG PET/CT is regarded as the most suitable imaging technique for DSRCT and helps to select patients with a metabolic response to induction chemotherapy for debulking surgery even in the absence of significant tumor shrinkage according to RECIST (*17,18*).

C-X-C motif chemokine receptor 4 (CXCR4) was first identified as a coreceptor for HIV (X4-tropic isolates) entry into cells. Beyond its role in various physiologic processes, including embryogenesis, angiogenesis, and modulation of hematopoietic stem cells (*19,20*), CXCR4 has gained attention because it is overexpressed in more than 20 different tumor entities (*21–24*), including sarcoma (*25–27*), with higher receptor expression denoting poor prognosis (*23,28,29*). In particular, among sarcomas, CXCR4 overexpression has been previously described in Ewing sarcoma, which shares many biologic features with DSRCT, providing a rationale for exploring and targeting CXCR4 in DSRCT (*26*). Recently, noninvasive visualization of CXCR4 in vivo using PET has become possible with the development of [^{68}Ga]pentixafor (*30*). In addition, the first proof-of-concept studies have demonstrated the feasibility of subsequent receptor-directed endoradiotherapy in CXCR4-expressing diseases (*21,31–33*).

MATERIALS AND METHODS

Inclusion of Patients

This case study was approved by the Ethics Committee of the Medical Faculty, University of Würzburg (approval 20201001 01), and written informed consent was obtained from all patients before diagnostic and therapeutic procedures. [^{68}Ga]pentixafor was offered in compliance with §37 of the Declaration of Helsinki and the German Medicinal Products Act Arzneimittelgesetz §13 2b.

Between October 2015 and April 2020, 8 young, male patients (median age at diagnosis, 29 y [range, 8–43 y]) with DSRCT (7 confirmed cases of DSRCT patients, 1 case of undifferentiated peritoneal small round cell sarcoma with clinical and morphologic features of DSRCT) underwent imaging with [^{18}F]FDG and [^{68}Ga]pentixafor PET/CT at our institution. At presentation, all patients had extensive disease, with Hayes–Jordan stage II (widespread intraabdominal lesions) in 2 patients, stage III (additional liver metastasis) in 1 patient, and stage IV (additional extraabdominal metastasis) in 5 patients (including 4 patients with liver metastasis; Table 1). Finally, 4 patients with advanced, unresectable, and progressive disease after conventional therapies were selected for CXCR4-directed [^{90}Y]endoradiotherapy and after individual dosimetry received a total of 5 cycles of endoradiotherapy.

Imaging Protocol and Analysis

All patients underwent CXCR4-directed PET/CT ([^{68}Ga]pentixafor, to noninvasively visualize the receptor expression of DSRCT lesions and evaluate eligibility for CXCR4-directed endoradiotherapy) and [^{18}F]FDG PET/CT (as a control). Both PET/CT studies were performed on 2 consecutive days (the supplemental materials, available at http://jnm.snmjournals.org, provide a detailed description) (*34*). Briefly, PET/CT images were independently analyzed by 2 nuclear medicine specialists using a commercial software package (syngo.via, VB60A HF02; Siemens Healthineers AG). All lesions with nonphysiologic uptake of the respective tracer higher than the physiologic background were rated as CXCR4-positive or [^{18}F]FDG-positive. For corresponding tumor lesions on [^{68}Ga]pentixafor and [^{18}F]FDG PET/CT, the average SUV_{max} within a spheric volume of 1 mL (SUV_{peak}) was recorded, and tumor-to-background ratios (TBRs) were calculated (details are provided in the supplemental materials) (*35*). For posttherapeutic tumor evaluation, [^{18}F]FDG PET/CT imaging was performed. Tumor response was assessed by [^{18}F]FDG PET/CT using RECIST 1.1 and PERCIST 1.0 (*36,37*).

TABLE 1
Patient Characteristics

Patient no.	Sex	Age (y)	Tumor sites/Hayes–Jordan stage	EWSR1-WT1	CXCR4-pos. tumor cells	Prior Tx lines (*n*)	HD-CT (ASCT)	CRS	ERT
1	M	8	PM, LN, LV, I; stage III	Pos.	80%	3	No	Yes, R2†	Yes
2	M	20	PM, LN, LV, SP, D, P, MT, A; stage IV	Pos.	95% (80%*)	4	No	No	Yes
3	M	26	PM, LN, I; stage II	Pos.	95%	4 + HD	Yes	Yes, CC 2 (+HIPEC)	Yes
4	M	31	PM, LN (cervical); stage IV	Pos.	70%	1	No	Yes‡, CC 2 (+HIPEC)	No
5	M	43	PM, ST; stage II	Neg.	0%	1	No	Yes‡, CC 1 (+HIPEC)	No
6	M	37	PM, LV, MT, A; stage IV	Pos.	80%	1 + HD	Yes	Yes‡, CC 1 (+HIPEC)	No
7	M	35	PM, LN, LV, ST, MT, A; stage IV	Pos.	70%	5	Yes (with ERT)	Yes, CC 1 (+HIPEC)	Yes
8	M	23	PM, LN, LV, SP, ST, BM; stage IV	Pos.	55%	1 + HD (focal RT)	Yes	Yes, CC 1 (+HIPEC)	No

*Postmortem biopsy after 2 cycles of ERT.
†Partial tumor debulking.
‡After diagnostic CXCR4 PET.
Tx = therapy; HD-CT = high-dose chemotherapy; ASCT = autologous stem cell transplantation; CRS = cytoreductive surgery; ERT = endoradiotherapy; PM = peritoneal manifestation; LN = lymph node metastases; LV = liver metastases; I = intestinal obstruction/infiltration; Pos. = positive; R2 = R2 resection (residual tumor); SP = spleen metastases; D = diaphragmatic infiltration; P = pleural metastases; MT = thoracic involvement/mediastinal tumor; A = ascites; HD = high-dose chemotherapy; CC = completeness-of-cytoreduction score; HIPEC = hyperthermic intraperitoneal chemotherapy; ST = soft-tissue metastases; BM = bone metastases; RT = radiation therapy.

Immunohistochemistry

In total, 9 biopsies from all 8 patients were examined for CXCR4 expression by immunohistochemistry (patient 2 had a second postmortem biopsy from a liver metastasis). The intensity of CXCR4 expression was visually rated using a 4-point scale (0, absent; 1, weak; 2, moderate; and 3, intense). The percentage of stained tumor cells was estimated, and the staining intensity was rated by the immunoreactive score (supplemental materials) (*38*).

CXCR4-Directed Therapy

For patients selected for CXCR4-directed endoradiotherapy, individual pretherapeutic dosimetry with [^{177}Lu]pentixather, with a mean activity of 180 ± 45 MBq, was performed as previously described (*39*). Achievable doses in the tumor manifestations were estimated by multiplying the calculated dose coefficient in Gy/GBq by the administered activity of [^{90}Y]pentixather. Standardized institutional protocols for the endoradiotherapy work-up were applied, as previously described (*21,33*). Drug-related adverse events and toxicities were evaluated according to the Common Toxicity Criteria of the National Cancer Institute (version 5.0) (*40*). Progression-free survival and OS were calculated from the date of endoradiotherapy until documented radiologic or clinical progression or death.

Statistical Analysis

Statistical analyses were performed using Prism, version 9.3.0 (GraphPad Software). Descriptive data are presented as mean ± SD or median and range. To test for a normal distribution, the Shapiro–Wilk test was applied and refuted a normal distribution in most of the imaging data (SUV and TBR). For statistical comparison of SUV and TBR for both tracers in corresponding lesions, as well as before and after therapy, the Wilcoxon signed-rank test was performed. *P* values of less than 0.05 were considered statistically significant.

RESULTS

Patient Cohort

The patient characteristics are detailed in Table 1 and the supplemental materials, and the treatment course is illustrated in Figure 1. Before CXCR4 imaging and subsequent endoradiotherapy (if the patient was eligible), all 8 patients received intensive multiagent induction chemotherapy according to established sarcoma protocols (e.g., EWING 2008 protocol) (*41–43*), followed by high-dose chemotherapy with autologous stem cell transplantation in analogy to Kushner et al. (3 patients) (*44*) or as conditioning chemotherapy along with endoradiotherapy (1 patient). A median of 2.5 lines (range, 1–5 lines) of previous systemic regimens were administered before CXCR4 imaging and subsequent endoradiotherapy. Seven patients underwent prior abdominal debulking surgery (6 with additional hyperthermic intraperitoneal chemotherapy), and 1 patient was subjected to radiation therapy of a single vertebral body before diagnostic CXCR4 PET. The median time from the start of first-line systemic therapy to endoradiotherapy was 15.1 mo (range, 7.3–33.4 mo), and the median interval between diagnostic CXCR4 PET and CXCR4-directed [^{90}Y]endoradiotherapy was 48 d (range, 26–92 d). Notably, patient 2 received 2 subsequent cycles of endoradiotherapy.

Analysis of [^{68}Ga]Pentixafor and [^{18}F]FDG PET

All 7 patients with EWSR1-WT1 fusion-positive DSRCT showed a significant accumulation of [^{68}Ga]pentixafor in tumor lesions, whereas patient 5, classified as having an undifferentiated sarcoma on reference pathology, was the only patient lacking tracer uptake. Although most of the tumor manifestations were concordantly CXCR4-positive and [^{18}F]FDG-positive, we found discordant [^{18}F]FDG-positive, CXCR4-negative manifestations in 3 patients (2 patients with only 1 lymph node metastasis and 1 patient with 3 peritoneal metastases). In contrast, discordant [^{18}F]FDG-negative, CXCR4-positive manifestations were observed in 3 patients (2 patients with only 1 metastasis [liver in one and lymph node in the other] and 1 patient with 3 peritoneal metastases). Figure 2 shows an example of patient 2. Of an overall 61 tumor lesions, 60 showed [^{18}F]FDG uptake (98.4%) and 57 showed [^{68}Ga]pentixafor uptake (93.4%). Fifty-six lesions showed corresponding [^{18}F]FDG and [^{68}Ga]pentixafor uptake. Of these, the median SUV_{peak} (5.7 [range, 1.5–16.6] vs. 4.7 [range, 1.7–10.3], $P \leq 0.001$) and median TBR (3.8 [range, 0.9–9.2] vs. 2.9 [range, 0.7–5.9], $P \leq 0.001$) were significantly higher for [^{18}F]FDG than for [^{68}Ga]pentixafor.

Individual Dosimetry and Therapy with [^{90}Y]Pentixather

After baseline screening with [^{68}Ga]pentixafor PET/CT, all except 1 patient (patient 5) were considered eligible for CXCR4-directed endoradiotherapy. However, after interdisciplinary counseling, patient 4 opted for in-label treatment with pazopanib, whereas patients 6 and 8 had to be excluded because of compliance reasons and insufficient uptake in [^{177}Lu]pentixather dosimetry, respectively. In the remaining patients, the mean estimated doses for tumor lesions were 2.7 ± 0.9 Gy/GBq (range, 1.4–3.6 Gy/GBq). Detailed dosimetry data are presented in Supplemental Table 1. Figure 3 shows an example of patient 7 before and after [^{90}Y]pentixather endoradiotherapy.

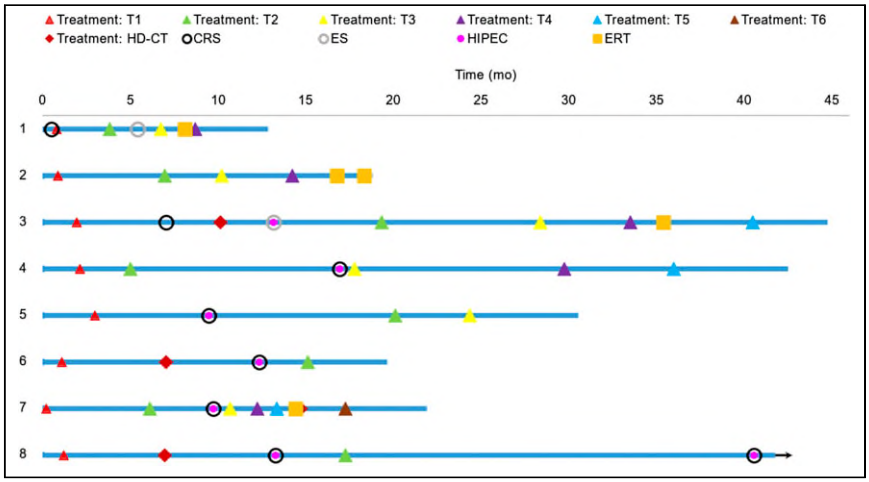

FIGURE 1. Swimmers plot for all patients from date of diagnosis until death. Systemic treatments are visualized by different symbols. Patient 8 is still alive, as indicated by arrow. CRS = cytoreductive surgery; ERT = CXCR-4 directed [^{90}Y]endoradiotherapy; ES = exploratory surgery; HD-CT = high-dose chemotherapy; HIPEC = hyperthermic intraperitoneal chemotherapy.

Safety

Four patients received a total of 5 cycles of [^{90}Y]pentixather with a mean activity of 6.6 ± 2.9 GBq (range, 1.7–9.1 GBq). Therapeutic administration of [^{90}Y]pentixather was well tolerated, and no severe nonhematologic adverse effects (≥grade 3 Common Terminology Criteria for Adverse Events) occurred. On day 3, patients were transferred from the Department of Nuclear Medicine

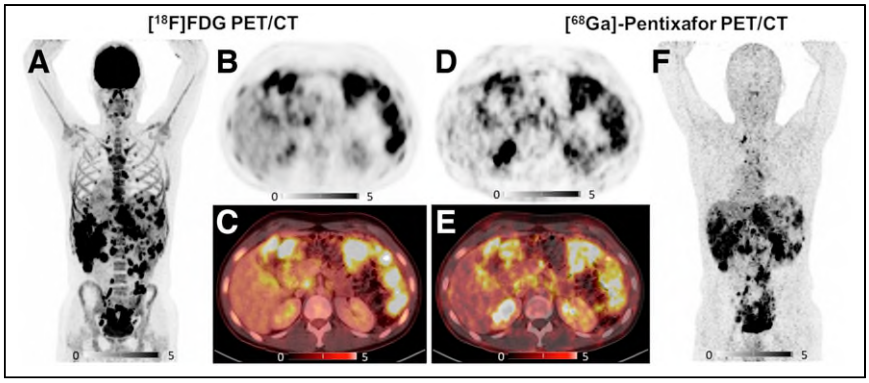

FIGURE 2. PET/CT scans with [^{68}Ga]pentixafor and [^{18}F]FDG for patient 2. (A–C) [^{18}F]FDG PET/CT shows intensive uptake in all tumor lesions (abdominal primary, lymph node, and hepatic metastasis) and moderate reactive uptake in bone marrow caused by chemotherapy. (D–F) In comparison, [^{68}Ga]pentixafor PET/CT demonstrates intensive and specific tracer accumulation in tumor lesions.

to Internal Medicine for further monitoring and autologous stem cell rescue on day 14 (after 5 half-lives of ^{90}Y).

Severe hematotoxicity was expected and occurred in all patients with myeloablative endoradiotherapy, resulting in grade 3–4 neutropenia (febrile neutropenia in 2 patients, onset from days 10–12), grade 4 thrombocytopenia (onset from days 10–18) requiring an average of 3 platelet concentrates, and prolonged grade 3–4 anemia requiring an average of 3 red blood cell units per patient to bridge the time until blood count recovery in all patients (Table 2). One patient with end-stage disease and preexisting obstructive jaundice from extensive liver metastases died of endoradiotherapy-induced neutropenia after the second treatment cycle from septic cholangitis on the day of planned stem cell rescue.

Antitumor Efficacy of Endoradiotherapy with [^{90}Y]Pentixather

Follow-up [^{18}F]FDG PET/CT demonstrated a significant decrease in the median SUV_{peak} after therapy (4.7 [range, 2.2–14.4] vs. 7.4 [range, 1.9–16.6], $P \leq 0.001$). In parallel, the median TBR also significantly declined (3.6 [range, 1.7–6.5] vs. 5.0 [range, 1.3–9.2], $P \leq 0.001$).

All 3 patients treated with myeloablative activity had signs of metabolic response, and 2 (patients 3 and 7) achieved stable disease according to RECIST. The third patient (patient 2) demonstrated a metabolic response in preexisting lesions but was classified as having PERCIST progressive disease because of new [^{18}F]FDG-positive lesions on the first follow-up imaging. This very frail patient with end-stage progressive disease and obstructive jaundice due to extensive liver metastases demonstrated indirect evidence of a response, with a temporary improvement in serum biochemistry, namely a 50% reduction in peak bilirubin levels after the first cycle of endoradiotherapy. Therefore, he continued to a second endoradiotherapy cycle but died from neutropenic sepsis 15 d after the second [^{90}Y] pentixather application, with no additional systemic chemotherapy applied. Notably, in this patient, evidence of regression in 30%–50% of tumor cells (fulfilling the pathologic partial-response criteria) was demonstrated on autopsy (Supplemental Fig. 1). Interestingly, the only patient in our endoradiotherapy cohort with no metabolic response had received a significantly reduced, nonmyeloablative [^{90}Y]pentixather activity because of lack of an autologous stem cell graft.

In summary, the progression-free survival of the cohort after endoradiotherapy was 104 d (range, 28–176 d), with the 2 evaluable patients demonstrating a promising progression-free survival of 143 and 176 d, respectively. Median OS of the total cohort from the start of first-line CT was 24.6 mo (range, 12.1–42.8 mo). This compares with survival data for DSRCT cohorts published in the literature, with OS varying between 24 and 29 mo (*8–10*).

Detailed information is summarized in Table 3 and the supplemental materials.

CXCR4 Immunohistochemistry

Moderate to strong membranous CXCR4 expression was detected by immunohistochemistry in 7 of 8 patients, with 55%–95% (median, 80%) positive cells. The immunoreactive score was predominantly in the middle range (6–8 points). Proliferative activity ranged from 20% to 70% (Ki-67), without association with CXCR4 labeling indices (Supplemental Table 2).

Patient 8 showed only 55% CXCR4-positive tumor cells, a finding that was associated with insufficient uptake during dosimetry. Patient 5, with morphologic and histologic features of DSRCT but no expression of EWSR1-WT1 fusion transcript, was classified as having undifferentiated sarcoma by reference pathology. This was the only patient completely negative for CXCR4 on immunohistochemistry and [^{68}Ga]pentixafor PET/CT. In patient 2, CXCR4 expression was also examined in the liver metastasis at autopsy after CXCR4 endoradiotherapy. Interestingly, CXCR4 expression level was still high (primary biopsy, 95%; autopsy material, 80%), and morphologically distinct signs of regression were present, with increased cell and nuclear pleomorphism as well as tumor necrosis (Supplemental Fig. 1).

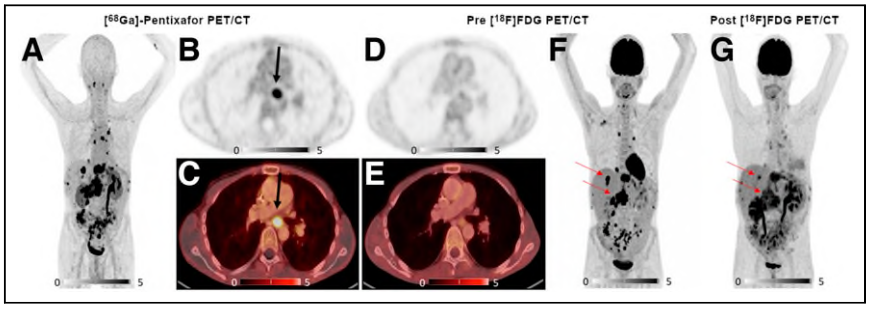

FIGURE 3. Pre- and posttherapeutic PET/CT scans with [^{68}Ga]pentixafor and [^{18}F]FDG for patient 7. Shown are pretherapeutic coronal (A) and axial (B and C) slices of PET/CT scan with [^{68}Ga]pentixafor and corresponding slices using [^{18}F]FDG (D–F). All metastatic lesions (lymph node, hepatic, and peritoneal implants) demonstrated intensive [^{68}Ga]pentixafor uptake with corresponding [^{18}F]FDG accumulation (F), except for 1 lymph node metastasis in mediastinum (B and C, black arrows). Posttherapeutic [^{18}F]FDG PET/CT shows significantly decreased metabolism of tumor lesions after [^{90}Y]pentixather therapy (G, red arrows).

DISCUSSION

Here, we report a cohort of 8 male patients with DSRCT who underwent imaging with [^{18}F]FDG and subsequent [^{68}Ga] pentixafor PET/CT as screening for potential

TABLE 2
Toxicities After CXCR4-Directed Endoradiotherapy

Parameter	Patient 1	Cycle 1	Cycle 2	Patient 3	Patient 7
		Patient 2			
Therapy activity (GBq)	1.7	7.2	9.1	6.6	8.2
Neutropenia	No	II	III	III	IV
Febrile neutropenia	No	No	Yes	No	Yes
Thrombocytopenia	No	IV	IV	III	IV
TC (units/3 mo)	No	3	2	3	3
Anemia (g/dL)	No	III	III	III	IV
RBC (units/3 mo)	No	2	2	4	4
AST (U/mL)	<ULN	I→II	II→II	I	I
Hyperbilirubinemia	<ULN	IV*	IV*	<ULN→3→ <ULN†	<ULN
Creatinine	I	<ULN	<ULN	<ULN	<ULN
Death (<3 mo after ERT)	No		Yes (neutropenic sepsis)	No	No

*Pretherapeutic jaundice due to obstructing liver metastasis.
†Preexisting liver fibrosis on elastography (FibroScan [Echosens]: F3–F4) resulting in temporary hyperbilirubinemia.
TC = thrombocyte concentrate transfusion; RBC = red blood cell transfusion; AST = aspartate aminotransferase; ULN = upper limit of normal; ERT = endoradiotherapy.

CXCR4-directed endoradiotherapy. CXCR4 expression has been previously described in different types of sarcoma, especially Ewing sarcoma, which shares many biologic features with DSRCT (*25–27*).

Radiation therapy is effective for DSRCT and has been shown to improve OS in some patients (*9,45,46*). However, whole-abdomen radiotherapy is associated with considerable toxicity in several organs at risk, resulting in significant dose reductions, and its benefits remain controversial. By leveraging the radiosensitive properties of DSRCT, we hypothesized that delivering radiotherapy on the molecular or cellular level targeting CXCR4 might reduce toxicity and offer a new treatment approach. CXCR4 endoradiotherapy has been shown to be safe and effective for different hematologic malignancies (*9,45*).

In our case series, we are the first—to our knowledge—to describe CXCR4 expression (confirmed by immunohistochemistry) in all cases of EWSR1-WT1 fusion-positive DSRCT. Notably, all these patients showed significant uptake of [^{68}Ga]pentixafor in their tumor lesions.

Comparative imaging with [^{18}F]FDG and [^{68}Ga]pentixafor PET/CT showed comparable detection rates of 98.4% for [^{18}F]FDG and 93.4% for [^{68}Ga]pentixafor PET/CT between the tracers, with sensitivity levels comparable to previously published data (*18*).

TABLE 3
Outcome After CXCR4-Directed Endoradiotherapy and Cause of Death

Patient no.	Max. calculated tumor dose (Gy)	ASCT (HD-CT)	RECIST	PERCIST	PFS from ERT (d)	OS from ERT (d)	OS from ICT (m)	Cause of death
1	6.1	No	PD	PD	65	143	12.1	Liver failure, small-bowel obstruction
2	25.2	ASCT d14	PD	PD*	28			
2	21.8	ASCT d14	NA	NA	NA†	61	18.0	Liver failure, cholangitis/sepsis in neutropenia
3	9.2	ASCT d14	SD	SD	143	282	42.8	Large-bowel obstruction, peritonitis/sepsis in neutropenia
7	21.3	ASCT d14 (Mel/Thio)	SD	PR	176	225	21.7	Small-bowel obstruction, gastrointestinal tumor bleeding, renal failure

*PD because of new lesions; otherwise, PR.
†Patient 2 died 15 d after second ERT.
Max. = maximum; ASCT = autologous stem cell transplantation; HD-CT = high-dose chemotherapy; PFS = progression-free survival; ERT = endoradiotherapy; ICT = induction chemotherapy; PD = progressive disease; d14 = day 14; NA = not applicable; SD = stable disease; PR = partial response; Mel = melphalan, 150 mg/m^2; Thio = thiotepa, 2 × 5 mg/kg.

Lesions with exclusive CXCR4 positivity or negativity likely represent tumor heterogeneity and may respond differently to treatment. These lesions should be monitored and further investigated by targeted biopsies and may offer potential for individualized treatment decisions, such as targeted irradiation or surgery.

Four of our patients were treated with CXCR4-directed [^{90}Y] endoradiotherapy after individual pretherapeutic dosimetry with [^{177}Lu]pentixather. In accordance with previous experience with CXCR4-directed endoradiotherapy in other entities (*21,31–33,47*), myelosuppression due to CXCR4 expression on hematopoietic cells requires obligatory stem cell rescue, blood product support, and management of febrile neutropenia. This expected hematotoxicity is manageable in a generally young, usually organ-fit DSRCT patient population.

Interestingly, metabolic activity was significantly decreased in tumor lesions after endoradiotherapy, as measured by [^{18}F]FDG PET/CT, indicating a therapeutic response (*17*). On a patient basis, 3 of 4 patients demonstrated signs of metabolic response, with the only nonresponder being probably underdosed (because of lack of stem cells). Remarkably, 2 patients with progressive disease before endoradiotherapy achieved disease stabilization with an OS of 225 and 282 d, respectively, and in the third patient, with fatal sepsis, a pathologic partial response was demonstrated on postmortem biopsy.

Promising results from an intraperitoneally applied radioligand (^{131}I-omburtamab) have been reported by others in DSRCT, with a superior OS of 54 mo as compared with historical data from the standard of care at 36 mo (*48*). However, this local therapy differs from our systemic treatment in 3 ways: only patients after cytoreductive surgery (i.e., without a measurable disease burden or with a low disease burden) were included, intraperitoneal radioimmunotherapy does not target extraabdominal disease, and almost all patients received additional whole-abdomen radiotherapy; thus, the effect of intraperitoneal radioimmunotherapy alone remains unclear. Supporting data were recently published, targeting fibroblast activation protein with ^{90}Y-labeled fibroblast activation protein inhibitor 46 radioligand therapy in a cohort that included 16 patients with advanced sarcoma (but no DSRCT). This approach was demonstrated to be safe and induced disease stabilization (RECIST 1.1) and metabolic responses (PERCIST) in approximately one third of the patients (*49*).

In our cohort, all treated patients presented with late-stage therapy-refractory DSRCT. We believe that more pronounced responses might be achievable with less tumor burden or an earlier disease stage. Given the descriptive and exploratory character of our analysis, we want to emphasize that our results have to be interpreted with caution and that the value of statistical analyses is severely compromised by the limited number of patients. However, considering the poor OS rates in DSRCT and the lack of standardized treatment, the medical need for innovative therapies is obvious. Thus, our proof-of-concept study could serve as a stimulus for future research and clinical trial design. For instance, we propose to investigate CXCR4 endoradiotherapy in DSRCT after early cytoreductive surgery or as part of a consolidating high-dose chemotherapy approach in patients with chemosensitive disease. In addition, modulation of CXCR4 receptor expression, as recently described by others (*50–52*), needs to be explored for its potential to increase endoradiotherapy efficacy. Finally, our promising data clearly indicate that CXCR4-directed endoradiotherapy may also be exploited in Ewing sarcoma, which occurs much more frequently and is known to overexpress CXCR4 (*26,53*).

CONCLUSION

CXCR4 is a promising diagnostic and therapeutic biomarker for DSRCT, as confirmed by immunohistochemistry and PET. We demonstrated the feasibility of CXCR4-directed endoradiotherapy and provided the first evidence of its antitumor activity.

DISCLOSURE

This work was supported by the IZKF Wuerzburg (grant Z-02/85 to Philipp Hartrampf). Hans-Jürgen Wester is a founder and shareholder of Scintomics. No other potential conflict of interest relevant to this article was reported.

KEY POINTS

QUESTION: Can CXCR4-directed endoradiotherapy be performed on DSRCT, a radiosensitive, yet difficult-to-treat sarcoma?

PERTINENT FINDINGS: Since DSRCT overexpresses CXCR4 on the cell surface, receptor-directed PET imaging and subsequent endoradiotherapy are feasible. Beyond the expected hematotoxicity, CXCR4-directed endoradiotherapy was well tolerated, with no severe nonhematologic adverse events, and was able to induce disease stabilization in patients with advanced DSRCT.

IMPLICATIONS FOR PATIENT CARE: CXCR4-directed endoradiotherapy in DSRCT is feasible and might prove a new option for patients with otherwise limited treatment alternatives.

REFERENCES

1. Lettieri CK, Garcia-Filion P, Hingorani P. Incidence and outcomes of desmoplastic small round cell tumor: results from the surveillance, epidemiology, and end results database. *J Cancer Epidemiol.* 2014;2014:680126.
2. Mello CA, Campos FAB, Santos TG, et al. Desmoplastic small round cell tumor: a review of main molecular abnormalities and emerging therapy. *Cancers (Basel).* 2021;13:498.
3. Hendricks A, Boerner K, Germer CT, Wiegering A. Desmoplastic small round cell tumors: a review with focus on clinical management and therapeutic options. *Cancer Treat Rev.* 2021;93:102140.
4. Negri T, Brich S, Bozzi F, et al. New transcriptional-based insights into the pathogenesis of desmoplastic small round cell tumors (DSRCTs). *Oncotarget.* 2017;8:32492–32504.
5. Slotkin EK, Bowman AS, Levine MF, et al. Comprehensive molecular profiling of desmoplastic small round cell tumor. *Mol Cancer Res.* 2021;19:1146–1155.
6. Subbiah V, Lamhamedi-Cherradi SE, Cuglievan B, et al. Multimodality treatment of desmoplastic small round cell tumor: chemotherapy and complete cytoreductive surgery improve patient survival. *Clin Cancer Res.* 2018;24:4865–4873.
7. Hayes-Jordan AA, Coakley BA, Green HL, et al. Desmoplastic small round cell tumor treated with cytoreductive surgery and hyperthermic intraperitoneal chemotherapy: results of a phase 2 trial. *Ann Surg Oncol.* 2018;25:872–877.
8. Scheer M, Vokuhl C, Blank B, et al. Desmoplastic small round cell tumors: multimodality treatment and new risk factors. *Cancer Med.* 2019;8:527–542.
9. Honoré C, Delhorme JB, Nassif E, et al. Can we cure patients with abdominal desmoplastic small round cell tumor? Results of a retrospective multicentric study on 100 patients. *Surg Oncol.* 2019;29:107–112.
10. Jeong H, Hong YS, Kim YH, et al. The role and clinical effectiveness of multiline chemotherapy in advanced desmoplastic small round cell tumor. *Clin Med Insights Oncol.* 2021;15:1179554920987107.
11. Italiano A, Kind M, Cioffi A, Maki RG, Bui B. Clinical activity of sunitinib in patients with advanced desmoplastic round cell tumor: a case series. *Target Oncol.* 2013;8:211–213.
12. Frezza AM, Benson C, Judson IR, et al. Pazopanib in advanced desmoplastic small round cell tumours: a multi-institutional experience. *Clin Sarcoma Res.* 2014;4:7.
13. Menegaz BA, Cuglievan B, Benson J, et al. Clinical activity of pazopanib in patients with advanced desmoplastic small round cell tumor. *Oncologist.* 2018;23:360–366.

14. Pasqualini C, Rubino J, Brard C, et al. Phase II and biomarker study of programmed cell death protein 1 inhibitor nivolumab and metronomic cyclophosphamide in paediatric relapsed/refractory solid tumours: arm G of AcSe-ESMART, a trial of the European Innovative Therapies for Children with Cancer Consortium. *Eur J Cancer.* 2021;150:53–62.
15. D'Angelo SP, Mahoney MR, Van Tine BA, et al. Nivolumab with or without ipilimumab treatment for metastatic sarcoma (Alliance A091401): two open-label, non-comparative, randomised, phase 2 trials. *Lancet Oncol.* 2018;19:416–426.
16. Tawbi HA, Burgess M, Bolejack V, et al. Pembrolizumab in advanced soft-tissue sarcoma and bone sarcoma (SARC028): a multicentre, two-cohort, single-arm, open-label, phase 2 trial. *Lancet Oncol.* 2017;18:1493–1501.
17. Ostermeier A, McCarville MB, Navid F, Snyder SE, Shulkin BL. FDG PET/CT imaging of desmoplastic small round cell tumor: findings at staging, during treatment and at follow-up. *Pediatr Radiol.* 2015;45:1308–1315.
18. Arora VC, Price AP, Fleming S, et al. Characteristic imaging features of desmoplastic small round cell tumour. *Pediatr Radiol.* 2013;43:93–102.
19. Luker GD, Yang J, Richmond A, et al. At the bench: pre-clinical evidence for multiple functions of CXCR4 in cancer. *J Leukoc Biol.* 2021;109:969–989.
20. Pawig L, Klasen C, Weber C, Bernhagen J, Noels H. Diversity and interconnections in the CXCR4 chemokine receptor/ligand family: molecular perspectives. *Front Immunol.* 2015;6:429.
21. Lapa C, Herrmann K, Schirbel A, et al. CXCR4-directed endoradiotherapy induces high response rates in extramedullary relapsed multiple myeloma. *Theranostics.* 2017;7:1589–1597.
22. Du W, Lu C, Zhu X, et al. Prognostic significance of CXCR4 expression in acute myeloid leukemia. *Cancer Med.* 2019;8:6595–6603.
23. Teixidó J, Martinez-Moreno M, Diaz-Martinez M, Sevilla-Movilla S. The good and bad faces of the CXCR4 chemokine receptor. *Int J Biochem Cell Biol.* 2018; 95:121–131.
24. Zhang Z, Ni C, Chen W, et al. Expression of CXCR4 and breast cancer prognosis: a systematic review and meta-analysis. *BMC Cancer.* 2014;14:49.
25. Oda Y, Tateishi N, Matono H, et al. Chemokine receptor CXCR4 expression is correlated with VEGF expression and poor survival in soft-tissue sarcoma. *Int J Cancer.* 2009;124:1852–1859.
26. Berghuis D, Schilham MW, Santos SJ, et al. The CXCR4-CXCL12 axis in Ewing sarcoma: promotion of tumor growth rather than metastatic disease. *Clin Sarcoma Res.* 2012;2:24.
27. Sun X, Charbonneau C, Wei L, Yang W, Chen Q, Terek RM. CXCR4-targeted therapy inhibits VEGF expression and chondrosarcoma angiogenesis and metastasis. *Mol Cancer Ther.* 2013;12:1163–1170.
28. Chatterjee S, Behnam Azad B, Nimmagadda S. The intricate role of CXCR4 in cancer. *Adv Cancer Res.* 2014;124:31–82.
29. Zhao H, Guo L, Zhao H, Zhao J, Weng H, Zhao B. CXCR4 over-expression and survival in cancer: a system review and meta-analysis. *Oncotarget.* 2015;6:5022–5040.
30. Demmer O, Gourni E, Schumacher U, Kessler H, Wester HJ. PET imaging of CXCR4 receptors in cancer by a new optimized ligand. *ChemMedChem.* 2011;6: 1789–1791.
31. Buck AK, Stolzenburg A, Hanscheid H, et al. Chemokine receptor-directed imaging and therapy. *Methods.* 2017;130:63–71.
32. Herrmann K, Schottelius M, Lapa C, et al. First-in-human experience of CXCR4-directed endoradiotherapy with ^{177}Lu- and ^{90}Y-labeled pentixather in advanced-stage multiple myeloma with extensive intra- and extramedullary disease. *J Nucl Med.* 2016;57:248–251.
33. Lapa C, Hanscheid H, Kircher M, et al. Feasibility of CXCR4-directed radioligand therapy in advanced diffuse large B-cell lymphoma. *J Nucl Med.* 2019;60:60–64.
34. Martin R, Juttler S, Muller M, Wester HJ. Cationic eluate pretreatment for automated synthesis of [^{68}Ga]CPCR4.2. *Nucl Med Biol.* 2014;41:84–89.
35. Landis JR, Koch GG. The measurement of observer agreement for categorical data. *Biometrics.* 1977;33:159–174.
36. Eisenhauer EA, Therasse P, Bogaerts J, et al. New response evaluation criteria in solid tumours: revised RECIST guideline (version 1.1). *Eur J Cancer.* 2009;45: 228–247.
37. Wahl RL, Jacene H, Kasamon Y, Lodge MA. From RECIST to PERCIST: evolving considerations for PET response criteria in solid tumors. *J Nucl Med.* 2009; 50(suppl 1):122S–150S.
38. Remmele W, Stegner HE. Recommendation for uniform definition of an immunoreactive score (IRS) for immunohistochemical estrogen receptor detection (ER-ICA) in breast cancer tissue. *Pathologe.* 1987;8:138–140.
39. Hänscheid H, Schirbel A, Hartrampf P, et al. Biokinetics and dosimetry of ^{177}Lu-pentixather. *J Nucl Med.* 2022;63:754–760.
40. Common Terminology Criteria for Adverse Events (CTCAE) version 5.0. Cancer Therapy Evaluation Program website. https://ctep.cancer.gov/protocoldevelopment/electronic_applications/docs/ctcae_v5_quick_reference_5x7.pdf. Published November 27, 2017. Accessed June 6, 2023.
41. Juergens C, Weston C, Lewis I, et al. Safety assessment of intensive induction with vincristine, ifosfamide, doxorubicin, and etoposide (VIDE) in the treatment of Ewing tumors in the EURO-E.W.I.N.G. 99 clinical trial. *Pediatr Blood Cancer.* 2006;47:22–29.
42. Strauss SJ, McTiernan A, Driver D, et al. Single center experience of a new intensive induction therapy for Ewing's family of tumors: feasibility, toxicity, and stem cell mobilization properties. *J Clin Oncol.* 2003;21:2974–2981.
43. Dirksen U, Brennan B, Le Deley MC, et al. High-dose chemotherapy compared with standard chemotherapy and lung radiation in Ewing sarcoma with pulmonary metastases: results of the European Ewing Tumour Working Initiative of National Groups, 99 Trial and EWING 2008. *J Clin Oncol.* 2019;37:3192–3202.
44. Kushner BH, LaQuaglia MP, Wollner N, et al. Desmoplastic small round-cell tumor: prolonged progression-free survival with aggressive multimodality therapy. *J Clin Oncol.* 1996;14:1526–1531.
45. Honoré C, Amroun K, Vilcot L, et al. Abdominal desmoplastic small round cell tumor: multimodal treatment combining chemotherapy, surgery, and radiotherapy is the best option. *Ann Surg Oncol.* 2015;22:1073–1079.
46. Kretschmar CS, Colbach C, Bhan I, Crombleholme TM. Desmoplastic small cell tumor: a report of three cases and a review of the literature. *J Pediatr Hematol Oncol.* 1996;18:293–298.
47. Habringer S, Lapa C, Herhaus P, et al. Dual targeting of acute leukemia and supporting niche by CXCR4-directed theranostics. *Theranostics.* 2018;8:369–383.
48. Modak S, Zanzonico P, Grkovski M, et al. B7H3-directed intraperitoneal radioimmunotherapy with radioiodinated omburtamab for desmoplastic small round cell tumor and other peritoneal tumors: results of a phase I study. *J Clin Oncol.* 2020; 38:4283–4291.
49. Fendler WP, Pabst KM, Kessler L, et al. Safety and efficacy of ^{90}Y-FAPI-46 radioligand therapy in patients with advanced sarcoma and other cancer entities. *Clin Cancer Res.* 2022;28:4346–4353.
50. Lapa C, Luckerath K, Kircher S, et al. Potential influence of concomitant chemotherapy on CXCR4 expression in receptor directed endoradiotherapy. *Br J Haematol.* 2019;184:440–443.
51. Weich A, Rogoll D, Gawlas S, et al. Wnt/β-catenin signaling regulates CXCR4 expression and [^{68}Ga] pentixafor internalization in neuroendocrine tumor cells. *Diagnostics (Basel).* 2021;11:367.
52. Rosenberg EM Jr, Harrison RES, Tsou LK, et al. Characterization, dynamics, and mechanism of CXCR4 antagonists on a constitutively active mutant. *Cell Chem Biol.* 2019;26:662–673.e7.
53. Jo VY. EWSR1 fusions: Ewing sarcoma and beyond. *Cancer Cytopathol.* 2020; 128:229–231.